Research article

Utilization of vanillin to prepare sulfated Calix[4]resorcinarene as efficient organocatalyst for biodiesel production based on methylation of palmitic acid and oleic acid

Jumina Jumina [**], Yehezkiel Steven Kurniawan [*], Ali Bahri Lubis, Eleonora Indira Larasati, Bambang Purwono, Sugeng Triono

Department of Chemistry, Faculty of Mathematics and Natural Sciences, Universitas Gadjah Mada, Yogyakarta 55281, Indonesia

A R T I C L E   I N F O

A B S T R A C T

Recently, biodiesel production from palm oils has been thoroughly investigated to substitute crude oil due to its scarcity. However, the biodiesel production process is time-consuming due to its slow kinetics; thus, concentrated sulfuric acid has been used to fasten the reaction process in some industries. Unfortunately, sulfuric acid is a toxic, corrosive, and non-environmentally friendly catalyst. In this study, we prepared sulfated Calix[4]resorcinarene derived from vanillin as an efficient organocatalyst to replace sulfuric acid. The catalytic activity of sulfated Calix[4]resorcinarenes was evaluated through the methylation of palmitic acid and oleic acid as model compounds due to their abundant amounts in palm oil. The Calix[4]resorcinarene and sulfated Calix[4]resorcinarenes have been obtained through a one-pot reaction in 71.8–98.3% yield. Their chemical structures were confirmed by using FTIR, NMR and HRMS spectrometry analyses. The results showed that the sulfated Calix[4]resorcinarene exhibited high catalytic activity for methyl palmitate and methyl oleate productions in 94.8 ± 1.8 and $97.3 \pm 2.1\%$ yield, respectively, which was comparable to sulfuric acid (96.3 ± 1.8 and $95.9 \pm 2.5\%$). The optimum condition was achieved by using 0.020 wt equivalent of organocatalyst for 6 h reaction process at 338 K. The methylation of palmitic acid and oleic acid fits well with the first-order kinetic model ($R^2 = 0.9940$–0.9999) with a reaction rate constant of 0.6055 and 1.1403 h^{-1}, respectively. Further investigation reveals that the hydroxyl group of vanillin plays a pivotal role in the organocatalytic activity of sulfated Calix[4]resorcinarene.

1. Introduction

Organocatalysis becomes a trending topic after Benjamin List and David MacMillan were awarded the Nobel prize in 2021. This era was begun with the report on organocatalyst-based proline and imidazolidinone molecules in the 20th century [1,2]. Organocatalyst is defined as a green catalyst composed of carbon, hydrogen, oxygen, nitrogen, sulfur, and/or phosphor elements [3] Organocatalysis offers a chemical reaction in a higher conversion within a faster reaction time. Additionally, organocatalyst agent is easier and cheaper to be prepared compared with inorganic catalysts, which is economically feasible for real application purposes [4]. The application of

  * Corresponding author.
 ** Corresponding author.
   E-mail addresses: jumina@ugm.ac.id (J. Jumina), yehezkiel.steven.kurniawan@mail.ugm.ac.id (Y.S. Kurniawan).

organocatalysts in the production of renewable energy attracts the researchers' attention due to the scarcity of crude oils in the future [5,6]. It was reported that the global supply of crude oils kept depleting year by year. Moreover, environmental pollution and its negative effects on human health led to serious concern about replacing crude oils for a better and sustainable world in the future [7]. In contrast, renewable energy from plant sources becomes the promising solution due to its abundant resources, cheaper mining cost, simpler mining technologies, and less impact on the environment [8,9].

Biodiesel is one of the renewable energies with some superior properties. Biodiesel is a biodegradable, non-toxic, and environmentally friendly energy due to its cleaner exhaust emission compared to petroleum diesel ones [10]. Biodiesel is produced through either the methylation of free fatty acids or the transesterification of triglycerides. Compared to the methylation of free fatty acids, the transesterification reaction is more complicated due to the stepwise conversion mechanism of triglycerides to glycerol and methyl esters [11]. Furthermore, the nature of plant oils depends on the geochemical and climate factors; thus, it is not easy to control and adjust as a standard comparison for literature purposes [12–15]. In contrast, methylation of free fatty acids is more preferable due to its exact physicochemical properties; thus, a faster and more efficient production process could be comprehensively studied.

According to Food and Agriculture Organization (FAO), Indonesia contributes 246 million tons of palm oil attributed to 60% of global demand in 2019, which is the highest global palm oil supply in the world [16]. In general, palm oil contains 38–44% of palmitic acid, 40–43% of oleic acid, 9–12% of linoleic acid, and 3–5% of stearic acid [17,18]. The Indonesian government have decided to blend petroleum diesel with biodiesel derived from palm oil, named as B35 policy, since 2023 [19]. Therefore, extensive research on biodiesel technology is carefully examined to establish efficient biodiesel production using palmitic acid and oleic acid as the model compounds.

Despite the advantages, large-scale biodiesel production is still far from industrial expectations due to its slow kinetics and poor conversion yield. Therefore, a highly active and efficient catalyst shall be utilized [20,21]. Tables 1 and 2 listed the catalytic activity of some reported catalysts for the methylation of palmitic acid and oleic acid, respectively. In general, inorganic catalysts gave medium to high yield for methyl palmitate (30.0–91.6%) and methyl oleate (55.3–98.0%), however, still lower than the use of organocatalysts. The catalytic efficiency of the inorganic catalysts (0.011–0.154 mol methyl palmitate/g and 0.027–0.098 mol methyl oleate/g) was also lower than the organocatalysts (0.002–0.173 mol methyl palmitate/g and 0.001–0.195 mol methyl oleate/g). Furthermore, the preparation of inorganic catalysts was not simple and expensive due to the usage of transition metals (such as zirconium, tungsten, titanium, and cerium).

Couples of organocatalysts for the methylation of palmitic acid and oleic acid have been reported [14,29–35,37,41–45]. Tables 1 and 2 showed that organocatalysts exhibit higher catalytic activity to produce methyl palmitate and methyl oleate in up to 98.3 and 97.6% yield, respectively. Compared to inorganic catalysts, organocatalysts offer several advantages such as being biodegradable, metal-free material, non-corrosive, no soap production, insensitive to water content, and having higher catalytic activity than other catalyst materials [10]. Biomolecules-based catalyst, i.e., Novozym 435, catalyzed the methylation of palmitic acid in 20.7% yield for 24 h at 333 K making its real application far from the reality due to their low yield, strict reaction condition, time-consuming, and expensive catalyst [30]. On the other hand, the *N*-methyl-*N*-butyl morpholine hydroxide ionic liquid produced methyl oleate in 62.4% yield. Even though the production yield of methyl oleate was moderate, however, the reaction time was too long (10 h) [42]. Another

Table 1

Comparison of the catalytic activity of some reported inorganic catalysts and organocatalysts for methyl palmitate production.

| No.	Catalyst	Yield (%)	Reaction time (h)	Temperature (K)	Efficiency (mol product/g catalyst)	Ref.
	Inorganic catalyst					
1	WO_x/ZrO_2	30.0	6	333	0.060	[22]
2	SBA-15/sulfated zirconia	40.0	6	333	0.027	[23]
3	Hβ zeolite	54.0	3	390	0.011	[24]
4	WS_2	70.0	6	333	0.070	[25]
5	Mesoporous Al-MCM-41	79.0	2	403	0.154	[26]
6	Sulfated zirconia	90.7	8	333	0.011	[27]
7	$C_7H_{13}N_2O_3S^+$ $H_2PW_{12}O_{40}^-$	91.6	8	338	0.051	[28]
	Organocatalyst					
8	Sulfated toluene	20.0	6	351	0.023	[29]
9	Novozym 435	20.7	24	333	0.002	[30]
10	Sulfated 4-hydroxybenzene	31.0	6	351	0.036	[29]
11	Sulfated alpha-cellulose	74.1	4	338	0.007	[31]
12	Sulfated *C*-phenylcalix[4]pyrogallolarene	83.0	4	338	0.150	[32]
13	Sulfated *C*-3,4-dimethoxyphenylcalix[4]pyrogallolarene	87.4	4	338	0.158	[32]
14	Sulfated calix[6]arene	90.0	6	351	0.164	[33]
15	Sulfated calix[4]arene	91.0	6	351	0.167	[33]
16	Sulfated *C*-4-hydroxy-3-methoxyphenylcalix[4]pyrogallolarene	91.9	4	338	0.168	[32]
17	Sulfated *C*-3,4-dimethoxyphenylcalix[4]-2-methylresorcinarene	93.3	6	338	0.165	[34]
18	Sulfated *C*-phenylcalix[4]-2-methylresorcinarene	96.3	6	338	0.170	[34]
19	Sulfated *C*-4-hydroxy-3-methoxyphenylcalix[4]-2-methylresorcinarene	97.8	6	338	0.173	[34]
20	Amberlite IR-120	98.3	10.5	334	0.038	[35]

Table 2

Comparison in the catalytic activity of some reported inorganic catalysts and organocatalysts for methyl oleate production.

No.	Catalyst	Yield (%)	Reaction time (h)	Temperature (K)	Efficiency (mol product/g catalyst)	Ref.
Inorganic catalyst						
1	Ceric ammonium sulfate	55.3	4	343	0.098	[36]
2	WO$_3$/USY	80.0	2	473	0.040	[37]
3	HZSM-5 zeolite	81.0	7	373	0.029	[38]
4	SiW$_{12}$/Hβ	86.0	10	333	0.027	[39]
5	Sulfated LaO	95.5	6	373	0.034	[38]
6	Sulfated Ce/ZrO$_2$–TiO$_2$	98.0	4	333	0.070	[40]
Organocatalyst						
7	Chitosan	00.9	5	368	0.001	[41]
8	Sulfated toluene	05.0	4	351	0.023	[33]
9	Sulfated 4-hydroxybenzene	48.0	4	351	0.024	[33]
10	Sulfated CMK-3	52.0	10	353	0.026	[39]
11	Sulfated Nafion	59.0	10	353	0.030	[39]
12	*N*-methyl-*N*-butyl morpholine hydroxide ionic liquid	62.4	10	333	0.044	[42]
13	Sulfated calix[6]arene	76.0	4	351	0.154	[33]
14	Sulfated alpha-cellulose	82.0	4	338	0.072	[31]
15	Sulfated calix[4]arene	88.0	4	351	0.195	[33]
16	Sulfated chitosan	95.7	5	368	0.113	[41]
17	Coal-based solid acid	97.6	6	513	0.058	[43]

biomaterial, i.e., chitosan, gave poor organocatalytic activity for methyl oleate production in 0.9% yield. However, the sulfated chitosan showed a remarkable production yield of methyl oleate at 95.7% [41]. The same trend has been reported for lanthanum(II) oxide (LaO) and alpha-cellulose catalysts. The bare LaO catalyst gave the methyl oleate in 80.0% yield while the sulfated LaO ones gave 95.5% yield [38]. On the other hand, sulfated alpha-cellulose gave a higher methylation yield of palmitic acid and oleic acid in 74.1 and 82.0% yield, respectively, compared to alpha-cellulose [31]. Sulfated aromatic-based organocatalysts have been also evaluated for the biodiesel production. Sulfated toluene yielded methyl palmitate and methyl oleate in 20.0 and 5.0% yield, respectively. On the other hand, sulfated 4-hydroxybenzene yielded the production of methyl palmitate and methyl oleate in 31.0 and 48.0% yield, respectively [29,33]. These results demonstrated that the presence of the hydroxyl group in the aromatic ring (named as phenolic derivative) enhanced the organocatalytic activity.

Cyclization of phenolic compounds could be performed to obtain calix[4]arene and calix[6]arene structures [46]. The sulfated calix[4]arene and calix[6]arene showed much higher production yield of methyl palmitate and methyl oleate in 90.0–91.0 and 76.0–88.0%, respectively, compared to their monomer, i.e., sulfated 4-hydroxybenzene (31.0–48.0%) due to the supramolecular interactions [29,33]. Unfortunately, the preparation of calix[4]arene and calix[6]arene is difficult and expensive because of complicated reaction and purification processes. Other calix[4]arene derivatives, i.e., calix[4]-2-methylresorcinarenes and calix[4]pyrogallolarenes, have been also investigated as organocatalysts for methyl palmitate production in our previous work [32,34]. They were successfully prepared through a one-pot reaction employing hydrochloric acid in ethanol media in 66.7–88.9% yield. The sulfated calix[4]-2-methylresorcinarenes gave a higher production yield of methyl palmitate (93.3–97.8%) than sulfated calix[4]pyrogallolarenes (83.0–91.9%). The catalytic efficiency of sulfated calix[4]-2-methylresorcinarene (0.165–0.173 mol/g) was also higher than sulfated calixarene (0.164–0.167 mol/g) and sulfated calix[4]pyrogallolarene (0.150–0.168 mol/g) for methyl palmitate production. Unfortunately, the production cost of sulfated calix[4]-2-methylresorcinarene was quite high due to the expensive 2-methylresorcinol as the starting material ($1910/kg). In contrast, resorcinol ($92/kg) is much cheaper than 2-methylresorcinol, however, the organocatalytic activity of sulfated Calix[4]resorcinarenes has not been studied yet.

In this work, we prepared sulfated Calix[4]resorcinarene from vanillin as the starting material due to its highly abundant and
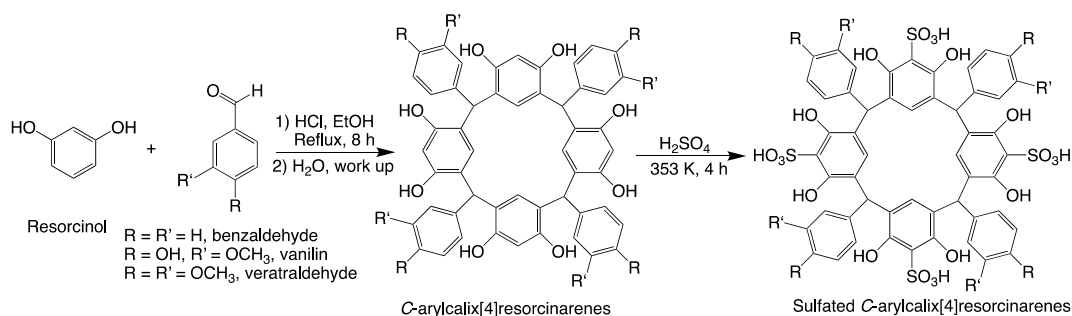
Scheme 1. Reaction scheme on the synthesis of sulfated Calix[4]resorcinarenes.

relatively cheap resources ($109/kg) in Indonesia [47]. Vanillin contains aldehyde, hydroxyl and methoxy groups; thus, could be cyclized to form the cyclic Calix[4]resorcinarene structure through a one-pot reaction. The role of hydroxyl and methoxy groups was evaluated by preparing the other sulfated Calix[4]resorcinarenes, i.e., sulfated *C*-phenylCalix[4]resorcinarene from benzaldehyde (for a representative compound with no hydroxyl and methoxy groups) and sulfated *C*-3,4-dimethoxyphenylCalix[4]resorcinarene (for a representative compound with no hydroxyl group). The reaction scheme for the synthesis of sulfated Calix[4]resorcinarenes is shown in Scheme 1. They were applied as the organocatalyst agent for the methylation of palmitic acid and oleic acid as the model compounds for biodiesel production (Scheme 2). The effect of reaction time and organocatalyst amount on the production of methyl palmitate and methyl oleate were investigated. Furthermore, the kinetic analysis was conducted and compared with concentrated sulfuric acid as the commercial catalyst for biodiesel production.

2. Experimental section

2.1. Materials

2.1.1. Reagents
The used chemicals, i.e., resorcinol, benzaldehyde, vanillin, 3,4-dimethoxybenzaldehyde, ethanol, concentrated hydrochloric acid (37% w/v), and concentrated sulfuric acid (98% w/v), for synthesizing sulfated Calix[4]resorcinarenes were obtained from Merck in pro analytical grade. The materials used for methyl ester production, i.e., palmitic acid, oleic acid, methanol, sodium hydroxide, ethyl acetate, and anhydrous sodium sulfate, were also purchased from Merck in pro analytical grade.

#### 2.1.2. Synthesis of Calix[4]resorcinarenes
The mixture of 1.65 g (15 mmol) of resorcinol and 2.28 g (15 mmol) of vanillin was dissolved in 30 mL ethanol. Then, 1.5 mL of conc. hydrochloric acid was added to the mixture and the mixture was refluxed for 8 h. Afterward, the mixture was cooled down to reach room temperature and then poured into 50 mL of distilled water. The residue was filtered and washed with a mixture of cold ethanol and distilled water until the filtrate reached neutral pH. The product was dried in a vacuum desiccator and characterized using FTIR and NMR analyses. The benzaldehyde and 3,4-dimethoxybenzaldehyde were used to prepare *C*-phenylCalix[4]resorcinarene and *C*-3,4-dimethoxyphenylCalix[4]resorcinarene, respectively, using a similar procedure for *C*-4-hydroxy-3-methoxyphenylCalix[4]resorcinarene.

2.1.3. Synthesis of sulfated Calix[4]resorcinarenes
As much as 2 mmol of *C*-4-hydroxy-3-methoxyphenylCalix[4]resorcinarene was reacted with 10 mL of concentrated sulfuric acid at 353 K for 4 h. Afterward, the mixture was cooled down to reach room temperature and then washed with a mixture of ethyl acetate and methanol in 3:2 volume ratio until the colorless filtrate was observed. The product was dried in a vacuum desiccator and characterized using FTIR, NMR, HRMS analyses. Furthermore, the sulfated *C*-4-hydroxyl-3-methoxyphenylCalix[4]resorcinarene was subjected to scanning electron microscope, isothermal nitrogen adsorption-desorption, particle size distribution, zeta potential, Brønsted and Lewis acid sites measurements. A similar method was employed to prepare sulfated *C*-phenylCalix[4]resorcinarene and sulfated *C*-3,4-dimethoxyphenylCalix[4]resorcinarene.

2.2. Instrumental measurements

The analytical balance (Libror EB-330 Shimadzu) and hotplate (Thermo Scientific) were used in the synthesis of sulfated Calix[4]resorcinarenes. The synthesized products were characterized by using melting point apparatus (Electrothermal 9100), Fourier transforms infrared (FTIR, Shimadzu Prestige 21), nuclear magnetic resonance (NMR, JEOL JNM ECZ500R/S1), and high-resolution mass spectrometer (HRMS, Thermo Scientific™ Q Exactive™ High-Resolution Mass Spectrometer). The HRMS analysis was performed using Hypersil Gold aQ 100 mm × 1 mm x 1.9 μm as the analytical column at 303 K with gradient elution of a mixture of 0.1% formic acid in water and 0.1% formic acid in acetonitrile at 40 μL/min flow. The surface morphology of the organocatalyst was recorded using a scanning electron microscope (SEM) on Phenom Desktop ProXL. The isothermal nitrogen adsorption-desorption employing the organocatalyst material was carried out using a Quantachrome Nova 2200e instrument at 77.35 K. The particle size distribution of the organocatalyst was determined using a laser scattering particle size distribution analyzer (Horiba LA-960) while the zeta potential measurement was conducted using Horiba SZ-100. The Brønsted and Lewis acid sites of the organocatalyst were measured from the vapor adsorption of ammonia and pyridine using a gravimetric method as reported previously [48]. The evaluation of the catalytic
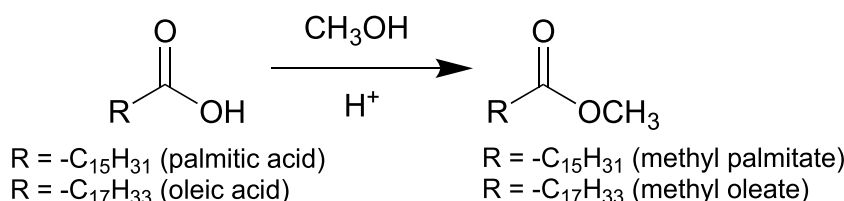
Scheme 2. Reaction scheme for the methylation of palmitic acid and oleic acid.

activity of sulfated Calix[4]resorcinarenes employed a rotary evaporator (Buchii R-114) and gas chromatography-mass spectrometry (GC-MS, Shimadzu-QP 2010S). The GC analysis was performed using Rtx 5 MS 30 m × 0.25 mm x 0.25 µm as the stationary phase at 573 K with helium gas as the mobile phase at 28 mL/min flow while the MS analysis used the electron ionization method at 70 eV.

2.3. Catalytic tests

First of all, palmitic acid (0.64 g, 2.5 mmol) was dissolved in methanol (10 mL, 250 mmol) with a methanol/palmitic acid molar ratio of 100. Then, the mixture was heated at 338 K in the presence of sulfated Calix[4]resorcinarene (0.05 mmol, 0.020 wt equivalent) as the organocatalyst. The reaction time was varied in 0.5, 1, 1.5, 2, 4 and 6 h to find the optimum reaction time. The zeroth-, first- and second-order kinetic models, as well as the Langmuir-Hinshelwood kinetic model, were then evaluated to determine the reaction rate constant. In another experiment, the organocatalyst amount was varied in 0.005, 0.010, 0.015, 0.020, 0.040, and 0.060 weight equivalent for the methylation reaction at 338 K for 6 h to find the optimum organocatalyst amount. After the reaction, the mixture was neutralized with 10% w/v sodium hydroxide solution and then extracted using ethyl acetate (3 × 10 mL). The organic phase was washed with distilled water (3 × 10 mL), dried over anhydrous sodium sulfate, and evaporated to remove the ethyl acetate. Investigation of methyl oleate production was carried out by replacing the palmitic acid (0.64 g, 2.5 mmol) with oleic acid (0.71 g, 2.5 mmol) in a molar ratio of methanol/oleic acid of 100. The experiment was performed in triplicate for each variation and the yield of methyl ester was shown as mean ± standard deviation. The methyl ester products were characterized using FTIR and GC-MS analyses.

3. Results and discussion

3.1. Synthesis and characterization of sulfated Calix[4]resorcinarenes

In this work, vanillin as an abundant natural resource in Indonesia was utilized as the starting material to prepare sulfated Calix[4] resorcinarene; thus, the production cost for this organocatalyst material could be reachable by the industries. Vanillin is a benzaldehyde derivative with hydroxy and methoxy groups at its para and meta positions. The effect of hydroxy and methoxy groups in vanillin on the organocatalytic activity was investigated by comparing the organocatalytic activity of the other sulfated Calix[4] resorcinarene with the absence of hydroxy and methoxy groups (sulfated C-phenylCalix[4]resorcinarene) and with the absence of hydroxy group (sulfated C-3,4-dimethoxyphenylCalix[4]resorcinarene). The reaction scheme is shown in Scheme 1. The synthesis process was conducted in a one-pot reaction between resorcinol and vanillin under acidic conditions. The reaction mechanism has been reported by Roberts et al. (2001) in investigating the formation of Calix[4]resorcinarene from resorcinol and benzaldehyde [49]. Briefly, the carbonyl of vanillin was protonated by hydrochloric acid to form the oxonium cation. The formation of the oxonium cation increases the electrophilicity of vanillin; thus, vanillin could react with resorcinol to form secondary alcohol as the intermediate. This alcohol was further protonated and attacked by another resorcinol to form the dimer. The reaction is completed when the tetramer unit was generated and this tetramer released water molecules as the byproducts to form the cyclic structure of Calix[4]resorcinarene.

The C-4-hydroxyl-3-methoxyphenylCalix[4]resorcinarene was obtained as a purplish powder in 71.8% yield from the reaction between resorcinol and vanillin. The melting point of this compound was 489–490 K. The high melting point of this compound (489–490 K) was caused by strong intermolecular hydrogen bonds in the solid state as reported earlier [49]. The FTIR spectrum of this compound showed the absorption signals at 3387, 2954 and 2846, 1612, 1427, and 1211 cm^{-1} for O–H, C–H methoxy, C]C aromatic, C–H methine, and C–O phenol and ether, respectively (Fig. S1). The presence of C–H methine as a sharp signal at 1427 cm^{-1} was observed in Fig. S1 suggesting that the structure of Calix[4]resorcinarene has been formed. The ^{1}H NMR spectrum of this compound was measured in DMSO-d_6 solvent with the data as follows: 8.36 (s, 8H, C$_6$H$_2$(O**H**)$_2$), 6.42, 6.33 and 6.13 (d ($J = 8.0$ Hz), d ($J = 8.0$ Hz) and s, 12H, C$_6$**H**$_3$(OH)(OCH$_3$)), 6.36 (s, 4H, C$_6$H$_3$(O**H**)(OCH$_3$)), 6.19, 6.08, 5.95 and 5.58 (s, s, s and s, 8H, C$_6$**H**$_2$(OH)$_2$), 5.41 (s, 4H, CH methine), and 3.39 (s, 12H, C$_6$H$_3$(OH)(OC**H**$_3$)) ppm (Fig. S2). The ^{1}H NMR spectrum of C-4-hydroxy-3-methoxyphenylCalix[4] resorcinarene confirmed the presence of all hydroxyl and aromatic protons. The hydroxyl groups from resorcinol were observed as a singlet signal at 8.36 ppm with an integral value of 8 protons. This integral value confirmed that the C-4-hydroxy-3-methoxyphenylCalix[4]resorcinarene contains four resorcinol aromatic structures as each resorcinol contains two hydroxyl protons. The aromatic protons from resorcinol were also observed as four singlet signals at 5.58–6.19 ppm showing that the C-4-hydroxy-3-methoxyphenylCalix[4]resorcinarene existed in partial cone conformation (C_{2v} point group) according to Ma et al. (2001) [50]. On the other hand, the aromatic protons from vanillin were found as one singlet at 6.13 ppm and two doublets at 6.33–6.42 ppm with a coupling constant of 8.0 Hz. Meanwhile, the hydroxyl and methoxy protons were observed as singlet signals at 6.36 (4H) and 3.39 (12H) ppm, respectively. The integral values confirmed that the C-4-hydroxy-3-methoxyphenylCalix[4]resorcinarene contains four vanillin aromatic structures as each vanillin contains a hydroxyl proton and three methoxy protons. The methine proton was found as a singlet signal at 5.41 ppm with an integral value of 4 protons confirming that each resorcinol and vanillin were connected with the methine bridge (Scheme 1).

On the other hand, the C-phenylCalix[4]resorcinarene was obtained as a brown powder in 90.9% yield from the reaction between resorcinol and benzaldehyde. The melting point of C-phenylCalix[4]resorcinarene was 494–495 K. Fig. S3 showed the FTIR spectrum of C-phenylCalix[4]resorcinarene. The absorption signals at 3387, 1612, 1427, and 1211 cm^{-1} correspond to O–H, C]C aromatic, C–H methine, and C–O phenol functional groups, respectively. The ^{1}H NMR spectrum of C-phenylCalix[4]resorcinarene in DMSO-d_6 showed signals at 8.57 (s, 8H, C$_6$H$_2$(O**H**)$_2$), 6.94 (s, 20H, C$_6$**H**$_5$), 6.74 and 6.13 (s and s, 8H, C$_6$**H**$_2$(OH)$_2$), and 5.62 (s, 4H, CH methine) ppm (Fig. S4). Meanwhile, C-3,4-dimethoxyphenylCalix[4]resorcinarene was obtained as a red powder in 95.4% yield from the reaction between resorcinol and 3,4-dimethoxybenzaldehyde. The melting point of this compound was 535 K. The FTIR spectrum of this

compound showed the absorption signals at 3425, 2954 and 2846, 1612, 1435, and 1211 cm^{-1} for O–H, C–H methoxy, C]C aromatic, C–H methine, and C–O phenol and ether, respectively (Fig. S5). The ^{1}H NMR spectrum of *C*-3,4-dimethoxyphenylCalix[4]resorci-narene in DMSO-d_6 showed signals at 8.43 (s, 8H, C$_6$H$_2$(O**H**)$_2$), 6.43, 6.18 and 6.13 (d (*J* = 8.0 Hz), d (*J* = 8.0 Hz) and s, 12H, C$_6$**H**$_3$(OCH$_3$)$_2$), 6.22 and 5.99 (s and s, 8H, C$_6$**H**$_2$(OH)$_2$), 5.42 (s, 4H, CH methine), 3.68 and 3.63 (s and s, 24H, C$_6$H$_3$(OC**H**$_3$)$_2$) ppm (Fig. S6). These spectroscopic data confirmed the successful formation of *C*-phenylCalix[4]resorcinarene and *C*-3,4-dimethox-yphenylCalix[4]resorcinarene.

Sulfated *C*-4-hydroxy-3-methoxyphenylCalix[4]resorcinarene was prepared from a sulfonation reaction using conc. sulfuric acid. The –SO$_3$H group was introduced on the aromatic ring of resorcinol rather than on the aromatic ring of vanillin due to its steric hindrance. Sulfated *C*-4-hydroxyl-3-methoxyphenylCalix[4]resorcinarene was obtained as a black powder in 97.3% yield. The melting point of this compound could not be determined as this compound was decomposed at 550 K. The FTIR spectrum of this compound showed the absorption signals at 3410, 2954, 1610, 1435, 1203, 1180, 856, and 578 cm^{-1} for O–H, C–H methoxy, C]C aromatic, C–H methine, C–O phenol and ether, S]O, S–O, and C–S, respectively, as shown in Fig. S7. The C–H methoxy, C]C aromatic, C–H methine, and C–O phenol and ether groups of *C*-4-hydroxy-3-methoxyphenylCalix[4]resorcinarene still existed in the FTIR spectrum demon-strating that these functional groups were not influenced during the sulfonation reaction. Meanwhile, the presence of sulfonic acid groups on the sulfated *C*-4-hydroxy-3-methoxyphenylCalix[4]resorcinarene was indicated by the presence of absorption signals for S]O, S–O, and C–S functional groups.

The ^{1}H NMR spectrum of sulfated *C*-4-hydroxy-3-methoxyphenylCalix[4]resorcinarene in DMSO-d_6 showed signals at 9.49 (s, 8H, C$_6$H(SO$_3$H)(O**H**)$_2$), 7.54, 6.97 and 6.81 (s, d (*J* = 8.5 Hz) and d (*J* = 8.5 Hz), 12H, C$_6$**H**$_3$(OH)(OCH$_3$)), 7.35 and 7.20 (s and s, 4H, C$_6$H (SO$_3$**H**)(OH)$_2$), 7.03 (s, 4H, C$_6$H$_3$(O**H**)(OCH$_3$)), 7.08 and 7.00 (s and s, 4H, C$_6$**H**(SO$_3$H)(OH)$_2$), 6.07 (s, 4H, CH methine), and 3.69 (s, 12H, C$_6$H$_3$(OH)(OC**H**$_3$)) ppm (Fig. S8). The protons of the C–H methoxy, C]C aromatic, C–H methine, and C–O phenol functional groups also remained in the ^{1}H NMR spectrum of sulfated *C*-4-hydroxy-3-methoxyphenylCalix[4]resorcinarene. Meanwhile, the protons of sulfonic acid were found as singlet signals at 7.35 and 7.20 ppm with an integral value of 4 protons. Further character-izations of sulfated *C*-4-hydroxy-3-methoxyphenylCalix[4]resorcinarene were performed using ^{13}C NMR and HRMS analyses. The ^{13}C NMR spectrum of sulfated *C*-4-hydroxy-3-methoxyphenylCalix[4]resorcinarene in DMSO-d_6 showed signals at 152, 137, 135 and 102 (aromatic carbons of C$_6$H(SO$_3$H)(OH)$_2$), 147, 144, 121, 114, 113 and 112 (aromatic carbons of C$_6$H$_3$(OH)(OCH$_3$)), 56 (methoxy carbon of C$_6$H$_3$(OH)(OCH$_3$)), and 41 (methine carbon) ppm (Fig. S9). The ^{13}C NMR spectrum of sulfated *C*-4-hydroxy-3-methoxyphenylCalix [4]resorcinarene showed a signal for methine carbon at 41 ppm, four aromatic carbons of sulfated resorcinol at a region of 102–152 ppm, and six aromatic carbons of vanillin were found at a region of 112–147 ppm. The HRMS analysis showed a signal at *m/z* = 1319.11 as C$_{56}$H$_{48}$NaO$_{28}$S$_4^+$ (M + Na$^+$).

Further characterization of sulfated *C*-4-hydroxy-3-methoxyphenylCalix[4]resorcinarene using SEM, isothermal nitrogen adsorption-desorption, particle size distribution, and zeta potential analyses have been performed. The SEM micrograph (Fig. 1(a)) revealed that the morphology of sulfated *C*-4-hydroxy-3-methoxyphenylCalix[4]resorcinarene was observed as aggregated irregular spherical particles in micrometer size. This phenomenon might be caused by strong intermolecular hydrogen bonds between sulfated *C*-4-hydroxy-3-methoxyphenylCalix[4]resorcinarenes. It was found that the surface area, pore volume and pore size of sulfated *C*-4-hydroxy-3-methoxyphenylCalix[4]resorcinarene was 9.51 m^2/g, 2.11 cm^3/g, and 19.68 nm, respectively. On the other hand, the average particle size of sulfated *C*-4-hydroxy-3-methoxyphenylCalix[4]resorcinarenes was 5.211 μm (Fig. 1(b)). The zeta potential of sulfated *C*-4-hydroxy-3-methoxyphenylCalix[4]resorcinarene was −32.0 mV because it contained O–H and O$_2$SO–H groups that could act as the proton donor. The Brønsted and Lewis acid sites of sulfated *C*-4-hydroxy-3-methoxyphenylCalix[4]resorcinarene were 12.28 and 3.50 mmol/g, respectively. The Brønsted acid site of sulfated *C*-4-hydroxy-3-methoxyphenylCalix[4]resorcinarene (12.28 mmol/ g) was higher than sulfated *C*-phenylCalix[4]resorcinarene (8.44 mmol/g) and sulfated *C*-3,4-dimethoxyphenylCalix[4]resorcinarene (7.56 mmol/g) due to the presence of additional hydroxyl group from vanillin. A similar trend was found for the Lewis acid site, the sulfated *C*-4-hydroxy-3-methoxyphenylCalix[4]resorcinarene had slightly higher Lewis acid sites (3.50 mmol/g) than sulfated *C*-phenylCalix[4]resorcinarene (3.04 mmol/g) and sulfated *C*-3,4-dimethoxyphenylCalix[4]resorcinarene (2.14 mmol/g). These acid
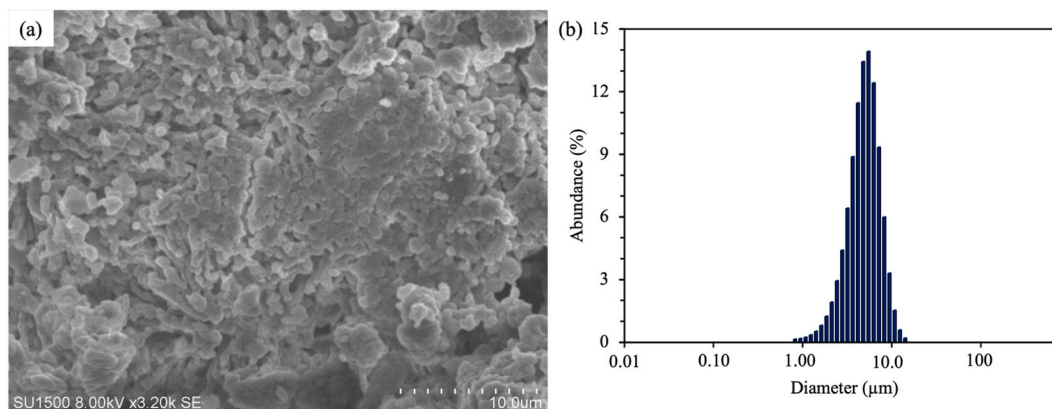

Fig. 1. (a) SEM morphology and (b) particle size distribution of sulfated C-4-hydroxy-3-methoxyphenylCalix[4]resorcinarene material.

sites could be utilized to catalyze the methylation reaction of either palmitic acid or oleic acid.

The sulfated C-phenylCalix[4]resorcinarene and sulfated C-3,4-dimethoxyphenylCalix[4]resorcinarene were also synthesized in this work to study the effect of hydroxyl and methoxy groups of vanillin on its organocatalytic activity. The sulfated C-phenylCalix[4]resorcinarene shows the absence of both hydroxyl and methoxy groups of vanillin while sulfated C-3,4-dimethoxyphenylCalix[4]resorcinarene shows the replacement of hydroxyl with methoxy group of vanillin. When the hydroxyl as proton donating group plays a pivotal role in the organocatalytic activity of methyl ester production; thus, the catalytic activity of sulfated C-4-hydroxy-3-methoxyphenylCalix[4]resorcinarene shall be higher than sulfated C-phenylCalix[4]resorcinarene and sulfated C-3,4-dimethoxyphenylCalix[4]resorcinarene. When the methoxy group is critical in the organocatalytic activity of methyl ester production; thus, the catalytic activity of sulfated C-3,4-dimethoxyphenylCalix[4]resorcinarene shall be higher than sulfated C-4-hydroxy-3-methoxyphenylCalix[4]resorcinarene and much higher than sulfated C-phenylCalix[4]resorcinarene. On the other hand, when both hydroxyl and methoxy groups of vanillin suppress the catalytic activity due to steric hindrance; thus, the catalytic activity of sulfated C-phenylCalix[4]resorcinarene shall be higher than sulfated C-3,4-dimethoxyphenylCalix[4]resorcinarene and sulfated C-4-hydroxy-3-methoxyphenylCalix[4]resorcinarene.

Sulfated C-phenylCalix[4]resorcinarene was obtained as a black powder in 81.7% yield. The melting point of this compound could not be determined as this compound was decomposed at 550 K. The FTIR spectrum of this compound showed the absorption signals at 3410, 1610, 1435, 1203, 1180, 856, and 578 cm^{-1} for O–H, C]C aromatic, C–H methine, C–O phenol, S]O, S–O, and C–S, respectively, as shown in Fig. S10. The ^{1}H NMR spectrum of sulfated C-phenylCalix[4]resorcinarene in DMSO-d_6 showed signals at 7.72 (s, 8H, C$_6$H (SO$_3$H)(O$\underline{H}$)$_2$), 7.52 (s, 20H, C$_6$$\underline{H}_5$), 7.18 (s, 4H, C$_6$$\underline{H}$(SO$_3$H)(OH)$_2$), 7.07 (s, 4H, C$_6$H(SO$_3$$\underline{H}$)(OH)$_2$), and 7.01 (s, 4H, CH methine) ppm (Fig. S11). While the ^{13}C NMR spectrum of this compound showed signals at 153, 144, 130 and 110 (aromatic carbons of C$_6$H(SO$_3$H) (OH)$_2$), 129, 127, 125 and 120 (aromatic carbons of C$_6$H$_5$), and 41 (methine carbon) ppm (Fig. S12). The HRMS analysis showed a signal at $m/z = 1135.09$ as C$_{52}$H$_{40}$NaO$_{20}$S$_4^+$ (M + Na$^+$). On the other hand, sulfated C-3,4-dimethoxyphenylCalix[4]resorcinarene was obtained as a black powder in 98.3% yield. The melting point of this compound could not be determined as this compound was decomposed at 550 K. The FTIR spectrum of this compound showed the absorption signals at 3348, 2906, 1627, 1435, 1203, 1165, 856, and 594 cm^{-1} for O–H, C–H methoxy, C]C aromatic, C–H methine, C–O phenol and ether, S]O, S–O, and C–S, respectively (Fig. S13). The ^{1}H NMR spectrum of sulfated C-3,4-dimethoxyphenylCalix[4]resorcinarene in DMSO-d_6 showed signals at 8.75 (s, 8H, C$_6$H(SO$_3$H)(O$\underline{H}$)$_2$), 7.54, 7.18 and 6.85 (s, d ($J = 8.5$ Hz) and d ($J = 8.5$ Hz), 12H, C$_6$$\underline{H}_3$(OCH$_3$)$_2$), 7.09 (s, 4H, C$_6$$\underline{H}$(SO$_3$H)(OH)$_2$), 6.96 (s, 4H, C$_6$H(SO$_3$$\underline{H}$)(OH)$_2$), 6.04 (s, 4H, CH methine), 3.72 and 3.71 (s and s, 24H, C$_6$H$_3$(OC$\underline{H}_3$)$_2$) ppm (Fig. S14). While the ^{13}C NMR spectrum of sulfated C-3,4-dimethoxyphenylCalix[4]resorcinarene in DMSO-d_6 showed signals at 152, 138, 121 and 102 (aromatic carbons of C$_6$H(SO$_3$H)(OH)$_2$), 148, 146, 120, 114, 113 and 110 (aromatic carbons of C$_6$H$_3$(OCH$_3$)$_2$), 56 and 55 (methoxy carbon of C$_6$H$_3$(OCH$_3$)$_2$), and 40 (methine carbon) ppm (Fig. S15). The HRMS analysis showed a signal at $m/z = 1375.17$ as C$_{60}$H$_{56}$NaO$_{28}$S$_4^+$ (M + Na$^+$). The spectroscopic analyses revealed that both sulfated C-phenylCalix[4]resorcinarene and sulfated C-3,4-dimethoxyphenylCalix[4]resorcinarene have been successfully synthesized.

3.2. Catalytic properties of sulfated Calix[4]resorcinarenes

The organocatalytic activity of sulfated Calix[4]resorcinarenes was investigated by varying reaction times, as well as by varying catalyst amounts to find the optimum condition. The effect of reaction time on the organocatalytic activity of sulfated Calix[4]resorcinarenes for methyl palmitate production is shown in Fig. 2. The sulfated C-4-hydroxy-3-methoxyphenylCalix[4]resorcinarene showed the highest production yield of methyl palmitate for 0.5–6 h of reaction time among the investigated organocatalysts. The production yield of methyl palmitate catalyzed by sulfated C-4-hydroxy-3-methoxyphenylCalix[4]resorcinarene (17.1 ± 0.5–87.4 ± 1.5%) was higher than sulfated C-phenylCalix[4]resorcinarene (11.5 ± 0.4–84.4 ± 2.1%) and much higher than sulfated C-3,4-dimethoxyphenylCalix[4]resorcinarene (5.8 ± 0.4–77.1 ± 2.1%). The production yield of methyl palmitate using sulfated C-4-hydroxy-3-methoxyphenylCalix[4]resorcinarene (17.1 ± 0.5–77.0 ± 1.5%) was also higher than sulfuric acid (6.2 ± 0.4–62.2 ± 1.1%)
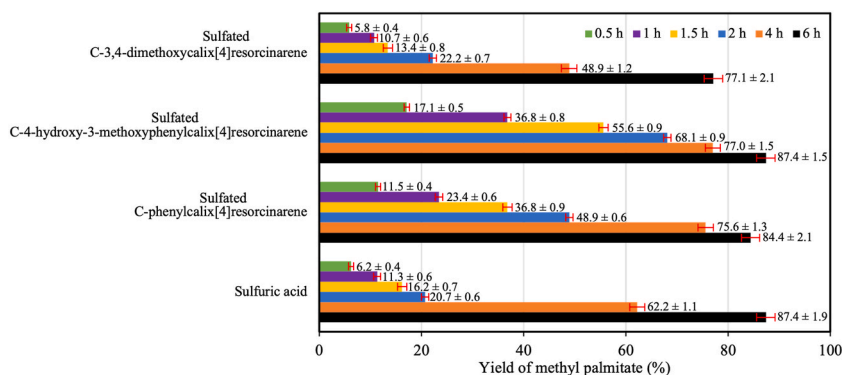

Fig. 2. Effect of reaction time on the organocatalytic activity of sulfated Calix[4]resorcinarenes for methyl palmitate production. Molar ratio of methanol/palmitic acid 100. Reaction temperature 338 K. Catalyst amount 0.02 weight equivalent.

for 0.05–4 h reaction time. While the production yield of methyl palmitate was comparable to sulfuric acid (87.4%) for 6 h of reaction time.

On the other hand, the effect of organocatalyst amount on the catalytic activity of sulfated Calix[4]resorcinarenes for methyl palmitate production is shown in Fig. 3. Again, the sulfated *C*-4-hydroxy-3-methoxyphenylCalix[4]resorcinarene showed the highest production yield of methyl palmitate amount among the investigated organocatalysts. The sulfated *C*-4-hydroxy-3-methoxyphenylCalix[4]resorcinarene exhibited a higher production yield of methyl palmitate (44.7 ± 0.7–94.8 ± 1.8%) than sulfated *C*-phenylCalix[4]resorcinarene (41.2 ± 0.5–87.4 ± 2.1%) and sulfated *C*-3,4-dimethoxyphenylCalix[4]resorcinarene (33.2 ± 0.6–77.1 ± 2.1%) for 0.005–0.060 wt equivalent. These experimental data revealed that the hydroxyl group plays a pivotal role in the organocatalytic activity of methyl palmitate production. In general, the optimum condition for the production of methyl palmitate was achieved using sulfated *C*-3,4-dimethoxyphenylCalix[4]resorcinarene and sulfated *C*-phenylCalix[4]resorcinarene at 0.020 wt equivalent for 6 h reaction time. Meanwhile, the optimum condition for sulfated *C*-4-hydroxy-3-methoxyphenylCalix[4]resorcinarene and sulfuric acid was achieved at 0.040 wt equivalent for 6 h of reaction time.

Since sulfated *C*-4-hydroxy-3-methoxyphenylCalix[4]resorcinarene showed the most efficient organocatalytic activity for methyl palmitate production, further investigation for the production of methyl oleate was carried out using this organocatalyst compound. The effect of reaction time on the organocatalytic activity of sulfated *C*-4-hydroxy-3-methoxyphenylCalix[4]resorcinarene for methyl oleate production is shown in Fig. 4. The sulfated *C*-4-hydroxy-3-methoxyphenylCalix[4]resorcinarene showed a higher production yield of methyl oleate for 0.5–6 h of reaction time compared to sulfuric acid, which was remarkable. On the other hand, Fig. 5 shows the effect of organocatalyst amount on the catalytic activity of sulfated *C*-4-hydroxy-3-methoxyphenylCalix[4]resorcinarene for methyl oleate production. The sulfated *C*-4-hydroxy-3-methoxyphenylCalix[4]resorcinarene showed the highest production yield of methyl oleate for 0.005–0.060 weight equivalents amount compared to sulfuric acid. The sulfated *C*-4-hydroxy-3-methoxyphenylCalix[4]resorcinarene at 0.06 weight equivalent for 6 h reaction time gave 97.3 ± 2.1% yield of methyl oleate.

The produced methyl palmitate and methyl oleate were characterized using FTIR, GC and MS analyses as shown in Fig. S16. The FTIR spectrum of methyl palmitate showed the absorption signals at 2924 and 2854, 1743, 1465, and 1242 cm^{-1} for C–H sp^3, C]O, C–H methylene, and C–O ester, respectively. The methyl palmitate was found as a single peak at a retention time (t_R) of 39.65 min confirming its 100% purity. The mass spectrum of methyl palmitate was measured using the electron ionization method and the fragments of methyl palmitate were observed as follows: 270 (M$^+$, 2%), 239 (2%), 227 (5%), 199 (2%), 185 (2%), 171 (2%), 157 (2%), 143 (10%), 129 (5%), 115 (3%), 101 (5%), 87 (65%), and 74 (100%). On the other hand, the FTIR spectrum of methyl oleate showed the absorption signals at 3001, 2924 and 2854, 1743, 1442, and 1172 cm^{-1} for C–H sp^2, C–H sp^3, C]O, C–H methylene, and C–O ester, respectively. The methyl oleate was also found as a single peak at t_R of 37.56 min confirming its 100% purity. The mass spectrum of methyl oleate showed the data as follows: 264 ([M-OCH$_3$]$^+$, 2%), 222 (2%), 180 (2%), 166 (2%), 137 (5%), 123 (10%), 97 (30%), 74 (50%), 69 (65%), and 55 (100%). These spectroscopic data agreed with the standards methyl palmitate and methyl oleate [31,51].

3.3. Catalytic efficiency of sulfated Calix[4]resorcinarenes

The catalytic efficiency of sulfated Calix[4]resorcinarenes was evaluated by comparing the reaction rate constant and the catalytic performance with other catalyst materials. The kinetic analysis for methyl palmitate production was performed based on the data in Fig. 2. Esterification reaction involves palmitic acid and methanol as the substrates. However, as the amount of methanol (250 mmol) was 100 times higher than palmitic acid (2.5 mmol); thus, the reaction kinetics in equation (1) could be simplified as Eq. (2) whereas k′ equals k [Methanol]^y.

$$-\frac{d[\text{Palmitic acid}]}{dt} = k\,[\text{Palmitic acid}]^x[\text{Methanol}]^y \tag{1}$$
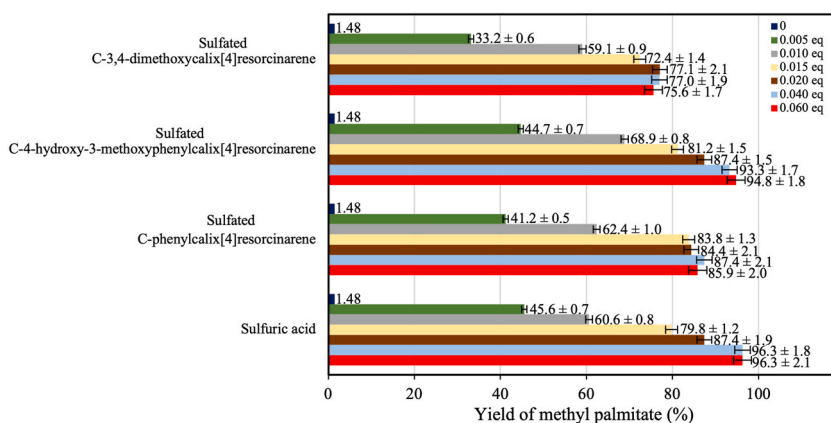

Fig. 3. Effect of organocatalyst amount on the catalytic activity of sulfated Calix[4]resorcinarenes for methyl palmitate production. Molar ratio of methanol/palmitic acid 100. Reaction temperature 338 K. Reaction time 6 h.
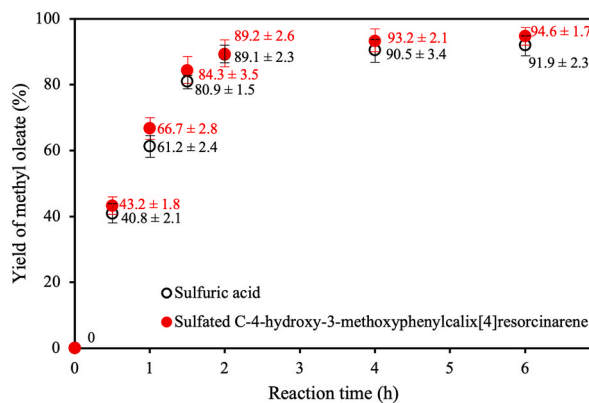
Fig. 4. Effect of reaction time on the organocatalytic activity of sulfated Calix[4]resorcinarenes for methyl oleate production. Molar ratio of methanol/oleic acid 100. Reaction temperature 338 K. Catalyst amount 0.02 weight equivalent.
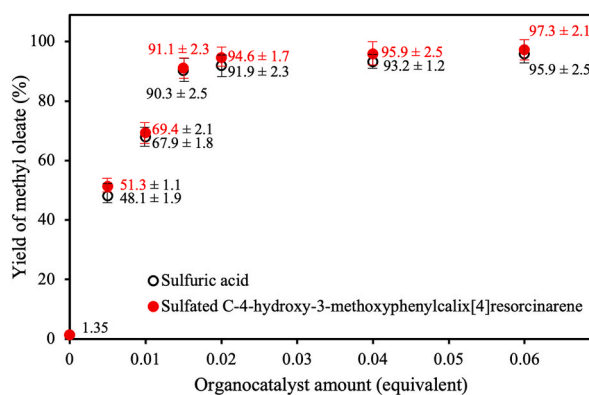

Fig. 5. Effect of organocatalyst amount on the catalytic activity of sulfated Calix[4]resorcinarenes for methyl oleate production. Molar ratio of methanol/oleic acid 100. Reaction temperature 338 K. Reaction time 6 h.

$$-\frac{d[\text{Palmitic acid}]}{dt} = k'[\text{Palmitic acid}]^x \tag{2}$$

Integration of Eq. (2) with n value of 0, 1 and 2 for zeroth-, first- and second-order kinetic model is shown in Eqs. (3)–(5), respectively.

$$[\text{Palmitic acid}]_t = -k't + [\text{Palmitic acid}]_0 \tag{3}$$

$$\ln [\text{Palmitic acid}]_t = -k't + \ln [\text{Palmitic acid}]_0 \tag{4}$$

$$\frac{1}{[\text{Palmitic acid}]_t} = k't + \frac{1}{[\text{Palmitic acid}]_0} \tag{5}$$

Additionally, the Langmuir-Hinshelwood kinetic model was also investigated, and the mathematical model is shown in Eq. (6):

$$\frac{-dt}{d[\text{Palmitic acid}]_t} = \frac{1}{k'} + \frac{1}{k'K[\text{Palmitic acid}]_t} \tag{6}$$

whereas K was the equilibrium constant for the adsorption of the substrate onto the organocatalyst material [52].

The kinetics analysis of methyl palmitate production using sulfated *C*-4-hydroxy-3-methoxyphenylCalix[4]resorcinarene is shown in Fig. 6. In general, the methylation of palmitic acid with solid acid catalysts followed the first-order kinetic model as previously reported [53,54]. The generation of methyl palmitate followed the first-order kinetic model, as reflected by the highest correlation factor ($R^2 = 0.9999$), with a mathematical equation of ln [Palmitic acid]$_t$ = −0.6055 Reaction time – 1.3918. Sulfuric acid catalysis also followed the first-order kinetic model with a mathematical equation of ln [Palmitic acid]$_t$ = −0.1153 Reaction time – 1.3895 ($R^2 = 0.9992$). The result showed that the reaction rate constant catalyzed by sulfated *C*-4-hydroxy-3-methoxyphenylCalix[4]resorcinarene ($k' = 0.6055$ h^{-1}) was 5.25 times higher than the sulfuric acid one ($k' = 0.1153$ h^{-1}). This phenomenon might be caused by high

Fig. 6. Kinetic analysis on the organocatalytic activity of sulfated Calix[4]resorcinarene for methyl palmitate production using (a) zeroth-order, (b) first-order, (c) second-order, and (d) Langmuir-Hinshelwood kinetic models. Molar ratio of methanol/palmitic acid 100. Reaction temperature 338 K. Catalyst amount 0.02 weight equivalent.

Brønsted and Lewis acid sites of sulfated *C*-4-hydroxy-3-methoxyphenylCalix[4]resorcinarene. Furthermore, sulfuric acid as a homogeneous catalyst is less preferable due to its non-environmentally friendly, toxic, and corrosive properties [55].

On the other hand, the kinetics analysis of the production of methyl oleate using sulfated *C*-4-hydroxy-3-methoxyphenylCalix[4]resorcinarene is shown in Fig. 7. It was reported that the methylation of oleic acid with other solid acid catalysts followed the first-order kinetic model as previously reported [42,56]. The methyl oleate production fits well with the first-order kinetic model, as reflected by the highest correlation factor ($R^2 = 0.9940$), with a mathematical equation of ln [Oleic acid]$_t$ = −1.1403 Reaction time − 1.3438. Catalysis using sulfuric acid also fits the first-order kinetic model with a R^2 value of 0.9926. It meant that the reaction rate constant catalyzed by sulfated *C*-4-hydroxy-3-methoxyphenylCalix[4]resorcinarene (k′ = 1.1403 h^{-1}) was slightly faster than the sulfuric acid one (k′ = 1.1061 h^{-1}), which was remarkable. This phenomenon could be caused by high Brønsted and Lewis acid sites.

The catalytic efficiency of sulfated *C*-4-hydroxy-3-methoxyphenylCalix[4]resorcinarene was 0.171 and 0.185 mol/g for the methylation reaction of palmitic acid and oleic acid, respectively. The catalytic efficiency of sulfated *C*-4-hydroxy-3-methoxyphenylCalix[4]resorcinarene is compared with other reported inorganic catalysts and organocatalysts for methyl palmitate and methyl oleate productions as listed in Tables 1 and 2 The sulfated *C*-4-hydroxy-3-methoxyphenylCalix[4]resorcinarene exhibited higher catalytic efficiency (0.171 mol/g) for methyl palmitate production than other inorganic catalysts such as WO$_x$/ZrO$_2$, SBA-15/ sulfated zirconia, Hβ zeolite, WS$_2$, mesoporous Al-MCM-41, functionalized phosphotungstic acid (C$_7$H$_{13}$N$_2$O$_3$S$^+$ H$_2$PW$_{12}$O$_{40}^-$), and sulfated zirconia (0.011–0.154 mol/g). This superior catalytic performance supported by simpler catalyst preparation than the inorganic catalysts making the sulfated *C*-4-hydroxy-3-methoxyphenylCalix[4]resorcinarene is promising for real application purposes. The catalytic efficiency of sulfated *C*-4-hydroxy-3-methoxyphenylCalix[4]resorcinarene (0.171 mol/g) was comparable to sulfuric acid (0.173 mol/g), however, sulfated *C*-4-hydroxy-3-methoxyphenylCalix[4]resorcinarene was better from the green chemistry and environmental point of views.

Compared to the other organocatalysts, sulfated *C*-4-hydroxy-3-methoxyphenylCalix[4]resorcinarene exhibited much higher catalytic efficiency (0.171 mol/g) than sulfated toluene, Novozym 435, sulfated 4-hydroxybenzene, sulfated alpha-cellulose, and Amberlite IR-120 (0.002–0.038 mol/g) for methyl palmitate production. Compared with the macrocyclic compounds, sulfated *C*-4-hydroxy-3-methoxyphenylCalix[4]resorcinarene also showed better catalytic efficiency (0.171 mol/g) than sulfated *C*-3,4-dimethoxyphenylCalix[4]resorcinarene, sulfated *C*-phenylcalix[4] pyrogallolarene, sulfated *C*-3,4-dimethoxyphenylcalix[4]pyrogallolarene, sulfated *C*-phenylCalix[4]resorcinarene, sulfated calix[6]arene, sulfated calix[4]arene, sulfated *C*-4-hydroxy-3-methoxyphenylcalix[4]pyrogallolarene, sulfated *C*-phenylcalix[4]-2-methylresorcinarene, and sulfated *C*-3,4-dimethoxyphenylcalix [4]-2-methylresorcinarene (0.150–0.170 mol/g). The organocatalytic trend for methyl palmitate production by using calix derivatives was found as follows, i.e., sulfated calix[4]arene (0.167 mol/g) < sulfated vanillin-based calix[4]pyrogallolarene (0.168 mol/g) <
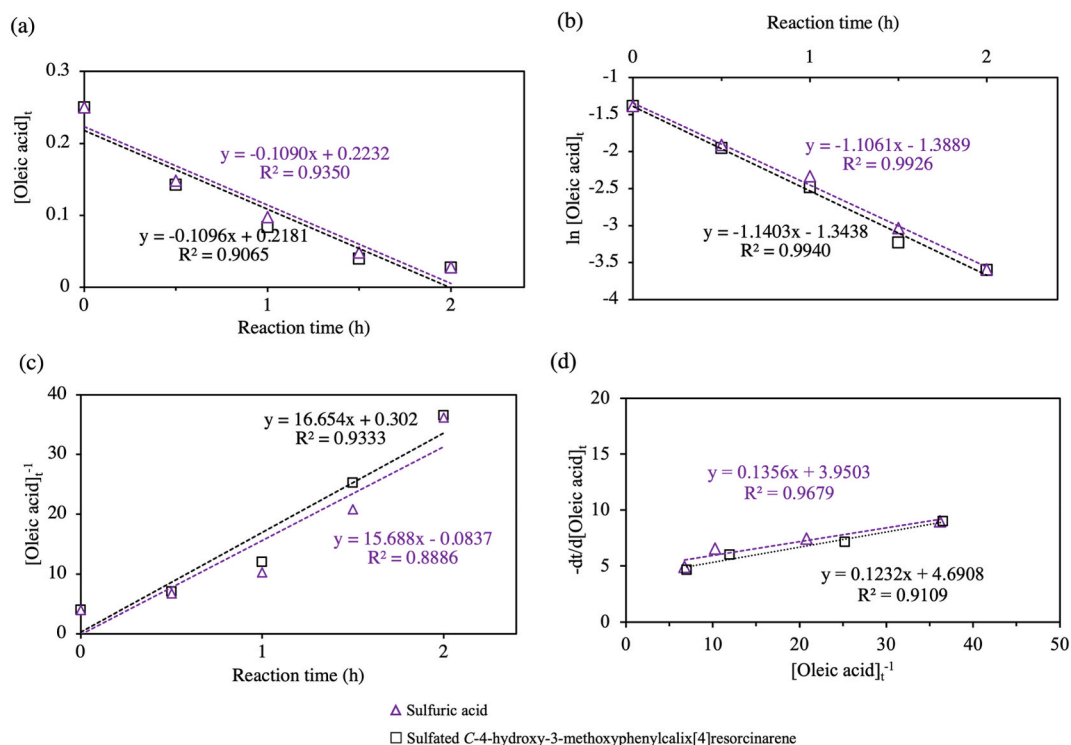
Fig. 7. Kinetic analysis on the organocatalytic activity of sulfated Calix[4]resorcinarenes for methyl oleate production using (a) zeroth-order, (b) first-order, (c) second-order, and (d) Langmuir-Hinshelwood kinetic models. Molar ratio of methanol/oleic acid 100. Reaction temperature 338 K. Catalyst amount 0.02 weight equivalent.

sulfated vanillin-based Calix[4]resorcinarene (0.171 mol/g) < sulfated vanillin-based calix[4]-2-methylresorcinarene (0.173 mol/g). The catalytic efficiency of sulfated *C*-4-hydroxy-3-methoxyphenylCalix[4]resorcinarene (0.171 mol/g) was slightly lower than sulfated *C*-4-hydroxy-3-methoxyphenylcalix[4]-2-methylresorcinarene (0.173 mol/g), however, the preparation cost for sulfated *C*-4-hydroxy-3-methoxyphenylcalix[4]-2-methylresorcinarene was much higher than the sulfated *C*-4-hydroxy-3-methoxyphenylCalix[4] resorcinarene ones demonstrating the advantage of using sulfated *C*-4-hydroxy-3-methoxyphenylCalix[4]resorcinarene as the organocatalyst.

On the other hand, the sulfated *C*-4-hydroxy-3-methoxyphenylCalix[4]resorcinarene yielded a higher catalytic efficiency (0.185 mol/g) than the other reported catalysts, i.e., ceric ammonium sulfate, WO_3/USY, HZSM-5 zeolite, SiW_{12}/Hβ, sulfated LaO, chitosan, sulfated toluene, sulfated 4-hydroxybenzene, sulfated CMK-3, sulfated Nafion, *N*-methyl-*N*-butyl morpholine hydroxide ionic liquid, sulfated alpha-cellulose, and sulfated chitosan (0.001–0.113 mol/g) for methyl oleate production. The sulfated *C*-4-hydroxy-3-methoxyphenylCalix[4]resorcinarene (0.185 mol/g) also exhibited higher catalytic efficiency than sulfuric acid (0.166 mol/g), which was remarkable. Additionally, the production yield of methyl oleate using sulfated *C*-4-hydroxy-3-methoxyphenylCalix[4]resorci-narene (97.3%) was close to the coal-based solid acid (97.6%) and sulfated Ce/ZrO_2–TiO_2 ones (98.0%) [40,43]. However, it shall be noted that the reaction temperature for using the coal-based solid acid catalyst was 1.5 times higher and the sulfated Ce/ZrO_2–TiO_2 required a complicated and costly preparation process. Furthermore, the catalytic efficiency of sulfated *C*-4-hydroxy-3-methox-yphenylCalix[4]resorcinarene (0.185 mol/g) was 3.2 and 2.6 higher than coal-based solid acid (0.058 mol/g) and sulfated Ce/Z-rO_2–TiO_2 (0.070 mol/g), respectively. Compared with the macrocyclic derivatives, sulfated *C*-4-hydroxy-3-methoxyphenylCalix[4] resorcinarene also showed a higher catalytic efficiency (0.185 mol/g) than sulfated calix[6]arene (0.154 mol/g) but lower than sulfated calix[4]arene (0.195 mol/g). However, the sulfated calix[4]arene required a higher reaction temperature (351 K) than the sulfated *C*-4-hydroxy-3-methoxyphenylCalix[4]resorcinarene (338 K) [33]. Therefore, this result demonstrates that sulfated *C*-4-hydroxy-3-methoxyphenylCalix[4]resorcinarene is a potential organocatalyst for the preparation of methyl palmitate and methyl oleate to substitute the sulfuric acid as the widely used catalyst in the future.

4. Conclusion

Organocatalysts based on Calix[4]resorcinarene and its sulfated derivative have been successfully prepared from resorcinol and vanillin in 71.8 and 97.3% yield. The chemical structures of the organocatalysts have been elucidated using FTIR, NMR and HRMS analyses. These organocatalysts showed high catalytic activity for methyl palmitate and methyl oleate productions in 94.8 ± 1.8 and 97.3 ± 2.1% yield, respectively. It was found that the hydroxyl group of vanillin plays a pivotal role in the methylation reaction of

palmitic acid and oleic acid. The production of methyl palmitate and methyl oleate followed the first-order kinetic model with a reaction rate constant of 0.6055 and 1.1403 h^{-1}, respectively. Compared to sulfuric acid as the commonly used catalyst, sulfated *C*-4-hydroxy-3-methoxyphenylCalix[4]resorcinarene exhibited comparable catalytic activity and efficiency to sulfuric acid for methyl esters production. However, sulfated *C*-4-hydroxy-3-methoxyphenylCalix[4]resorcinarene is a more efficient organocatalyst for real application purposes of biodiesel production to replace sulfuric acid due to its toxic and corrosive properties.

Author contribution statement

Jumina Jumina: Conceived and designed the experiments; Contributed reagents, materials, analysis tools or data.
Yehezkiel Steven Kurniawan: Performed the experiments; Analyzed and interpreted the data; Wrote the paper.
Ali Bahri Lubis, Eleonora Indira Larasati: Performed the experiments; Analyzed, and interpreted the data.
Bambang Purwono, Sugeng Triono: Conceived and designed the experiments.

Funding statement

Data availability statement

The data are available from the authors upon reasonable request.

Declaration of competing interest

The authors declare that they have no known competing financial interests or personal relationships that could have appeared to influence the work reported in this paper.

Appendix A. Supplementary data

Supplementary data to this article can be found online at https://doi.org/10.1016/j.heliyon.2023.e16100.

References

[1] D.W.C. MacMillan, The advent and development of organocatalysis, Nature 455 (2008) 304–308, https://doi.org/10.1038/nature07367.
[2] T. Ooi, C. Crudden, 2021 Nobel laurates recognized in organocatalysis, ACS Catal. 11 (2021), 15234, https://doi.org/10.1021/acscatal.1c05384.
[3] M.P. Helm, B. Klemm, R. Eelkema, Organocatalysis in aqueous media, Nat. Rev. Chem 3 (2019) 491–508, https://doi.org/10.1038/s41570-019-0116-0.
[4] V.G. Oliveira, M.F.C. Cardoso, L.S.M. Forezi, Organocatalysis: a brief overview on its evolution and applications, Catalysts 8 (2018) 605, https://doi.org/10.3390/catal8120605.
[5] B. Maleki, S.S.A. Talesh, M. Mansouri, Comparison of catalysts types performance in the generation of sustainable biodiesel via transesterification of various oil sources: a review study, Mater. Today Sustain. 18 (2022), 100157, https://doi.org/10.1016/j.mtsust.2022.100157.
[6] K.V. Ragavan, O. Hernandez-Hernandez, M.M. Martinez, T.J. Gutierrez, Organocatalytic esterification of polysaccharides for food applications: a review, Trends Food Sci. Technol. 119 (2022) 45–56, https://doi.org/10.1016/j.tifs.2021.11.028.
[7] K. Lang, B.R. Auer, The economic and financial properties of crude oil: a review, North Am. J. Econ. Finance 52 (2020), 100914, https://doi.org/10.1016/j.najef.2019.01.011.
[8] R.D. Sarkar, H.B. Singh, M.C. Kalita, Enhanced lipid accumulation in microalgae through nanoparticle-mediated approach, for biodiesel production: a mini-review, Heliyon 7 (2021), e08057, https://doi.org/10.1016/j.heliyon.2021.e08057.
[9] H.W. Aparamarta, S. Gunawan, S.I. Ihsanpuro, I. Safawi, D.S. Bhuana, A.F. Mochtar, M.Y.I. Noer, Optimization and kinetic study of biodiesel production from nyamplung oil with microwave-assisted extraction (MAE) technique, Heliyon 8 (2022), e10254, https://doi.org/10.1016/j.heliyon.2022.e10254.
[10] P. Maheshwari, M.B. Haider, M. Yusuf, J.J. Klemes, A. Bokhari, M. Beg, A. Al-Othman, R. Kumar, A.K. Jaiswal, A review on latest trends in cleaner biodiesel production: role of feedstock, production methods, and catalysts, J. Clean. Prod. 355 (2022), 131588, https://doi.org/10.1016/j.jclepro.2022.
[11] S. Bhattacharyya, Transesterification of yellow oleander seed oil, its utilization as biodiesel and performance evaluation, Heliyon 8 (2022), e09250, https://doi.org/10.1016/j.heliyon.2022.e09250.
[12] F. Ishola, D. Adelekan, A. Mamudu, T. Abodunrin, A. Aworinde, O. Olantunji, S. Akinlabi, Biodiesel production from palm olein: a sustainable bioresource for Nigeria, Heliyon 6 (2020), e03725, https://doi.org/10.1016/j.heliyon.2020.e03725.
[13] H. Helmiyati, Y. Budiman, G.H. Abbas, F.W. Dini, M. Khalil, Highly efficient synthesis of biodiesel catalyzed by a cellulose@hematite-zirconia nanocomposite, Heliyon 7 (2021), e06622, https://doi.org/10.1016/j.heliyon.2021.e06622.
[14] F. Febriani, N. Aura, P. Kemala, N. Saidi, T.M. Iqbalsyah, Novel thermostable lipase produced by a thermos-halophilic bacterium that catalyses hydrolytic and transesterification reactions, Heliyon 6 (2020), e04520, https://doi.org/10.1016/j.heliyon.2020.e04520.
[15] R. Djayasinga, A. Setiawan, A. Purnomo, A.Z. Amien, H. Hartanti, Utilization of breed chicken eggshells for biodiesel preparation from waste cooking oil, J. Multidiscip. Appl. Nat. Sci. 2 (2022) 41–46, https://doi.org/10.47352/jmans.2774-3047.90.
[16] FAO, World Food and Agriculture – Statistical Yearbook 2021. Rome, 2021, https://doi.org/10.4060/cb4477en.
[17] Z. Zulqarnain, M. Ayoub, M.H.M. Yusoff, M.H. Nazir, I. Zahid, M. Ameen, F. Sher, D. Floresyona, E.B. Nursanto, A comprehensive review on oil extraction and biodiesel production technologies, Sustainability 13 (2021) 788, https://doi.org/10.3390/su13020788.

[18] Y.S. Kurniawan, M. Anwar, T.D. Wahyuningsih, New lubricant from used cooking oil: cyclic ketal of ethyl 9,10-dihydroxyoctadecanoate, Mater. Sci. Forum 901 (2017) 135–141. https://dx.doi.org/10.4028/www.scientific.net/MSF.901.135.

[19] A.F. Widrian, B.S. Arifianto, N. Nurbaiti, N.A. Sasongko, Review of biodiesel policy in Indonesia, IOP Conf. Ser. Earth Environ. Sci. 1034 (2022), 012062, https://doi.org/10.1088/1755-1315/1034/1/012062.

[20] M. Athar, S. Zaidi, A review of the feedstocks, catalysts, and intensification techniques for sustainable biodiesel production, J. Environ. Chem. Eng. 8 (2020), 104523, https://doi.org/10.1016/j.jece.2020.104523.

[21] B. Changmai, C. Vanlalveni, A. Ingle, R. Bhagat, S.L. Rokhum, Widely used catalysts in biodiesel production: a review, RSC Adv. 10 (2020) 41625–41679, https://doi.org/10.1039/D0RA07931F.

[22] V.C. dos Santos, K. Wilson, A.F. Lee, S. Nakagaki, Physicochemical properties of WO_x/ZrO_2 catalysts for palmitic acid esterification, Appl. Catal. B Environ. 162 (2015) 75–84, https://doi.org/10.1016/j.apcatb.2014.06.036.

[23] A. Osatiashtiani, L.J. Durndell, J.C. Manayil, A.F. Lee, K. Wilson, Influence of alkyl chain length on sulfated zirconia catalyzed batch and continuous esterification of carboxylic acids by light alcohols, Green Chem. 18 (2016) 5529–5535, https://doi.org/10.1039/C6GC01089J.

[24] N.G. Grigoreva, A.M. Suleimanova, M.R. Agliullin, B.I. Kupetov, Synthesis of carboxylic esters in the presence of micro- and mesoporous aluminosilicates, Russ. J. Appl. Chem. 87 (2014) 773–779, https://doi.org/10.1134/S1070427214060184.

[25] V.C. dos Santos, L.J. Durndell, M.A. Isaacs, C.M.A. Parlett, K. Wilson, A.F. Lee, A new application for transition metal chalcogenides: WS_2 catalysed esterification of carboxylic acids, Catal. Commun. 91 (2017) 16–20, https://doi.org/10.1016/j.catcom.2016.12.003.

[26] A.C. Carmo Jr., L.K.C. de Souza, C.E.F. da Costa, E. Longo, J.R. Zamian, G.N.R. Filho, Production of biodiesel by esterification of palmitic acid over mesoporous aluminosilicate Al-MCM-41, Fuel 88 (2009) 461–468, https://doi.org/10.1016/j.fuel.2008.10.007.

[27] B. Banarjee, S. Bhunia, A. Bhaumik, Self-assembled sulfonated zirconia nanocrystals with mesoscopic void space synthesized via ionic liquid as a porogen and its catalytic activity for the synthesis of biodiesels, Appl. Catal., A 502 (2015) 380–387, https://doi.org/10.1016/j.apcata.2015.06.028.

[28] Y. Wang, D. Zhao, G. Chen, S. Liu, N. Ji, H. Ding, J. Fu, Preparation of phosphotungstic acid based poly(ionic liquid) and its application to esterification of palmitic acid, Renew. Energy 133 (2019) 317–324, https://doi.org/10.1016/j.renene.2018.10.029.

[29] S.A. Fernandes, R. Natalino, M.J. da Silva, C.F. Lima, A comparative investigation of palmitic acid esterification over *p*-sulfonic acid calix[4]arene and sulfuric acid catalysts via ^{1}H-NMR spectroscopy, Catal. Commun. 26 (2012) 127–131, https://doi.org/10.1016/j.catcom.2012.05.007.

[30] S. Sherkhanov, T.P. Korman, S.G. Clarke, J.U. Bowie, Production of FAME biodiesel in *E. coli* by direct methylation with an insect enzyme, Sci. Rep. 6 (2016), 24239, https://doi.org/10.1038/srep24239.

[31] J. Jumina, Y. Yasodhara, S. Triono, Y.S. Kurniawan, Y. Priastomo, H.M. Chawla, N. Kumar, Preparation and evaluation of alpha-cellulose sulfate based new heterogeneous catalyst for production of biodiesel, J. Appl. Polym. Sci. 138 (2020), 49658, https://doi.org/10.1002/app.49658.

[32] J. Jumina, H.R. Setiawan, S. Triono, Y.S. Kurniawan, D. Siswanta, A.K. Zulkarnain, N. Kumar, The *C*-Arylcalix[4]pyrogallolarene sulfonic acid: a novel and efficient organocatalyst material for biodiesel production, Bull. Chem. Soc. Jpn. 93 (2020) 252–259, https://doi.org/10.1246/bcsj.20190275.

[33] S.A. Fernandes, R. Natalino, P.A.R. Gazolla, M.J. da Silva, G.N. Jham, *p*-Sulfonic acid calix[n]arenes as homogeneous and recyclable organocatalysts for esterification reactions, Tetrahedron Lett. 53 (2012) 1630–1633, https://doi.org/10.1016/j.tetlet.2012.01.078.

[34] J. Jumina, I. Amalina, S. Triono, Y.S. Kurniawan, Y. Priastomo, K. Ohto, B.M. Yamin, Preliminary investigation of organocatalyst activity based on C-arylcalix[4]-2-methylresorcinarene sulfonic acid materials for biodiesel production, Bull. Kor. Chem. Soc. 42 (2021) 403–409, https://doi.org/10.1002/bkcs.12194.

[35] T. Dang, B. Chen, Optimization in esterification of palmitic acid with excess methanol by solid acid catalyst, Fuel Process. Technol. 109 (2013) 7–12, https://doi.org/10.1016/j.fuproc.2012.12.013.

[36] X. Long, L. Jian, Y. Lina, S. Yumeng, D. Jiali, Study on synthesis of butyl oleate catalyzed by ceric ammonium sulfate, Int. J. Sci. Eng. Res. 4 (2013) 1909–1911.

[37] A.A. Costa, P.R.S. Braga, J.L.D. Macedo, J.A. Dias, S.C.L. Dias, Structural effects of WO_3 incorporation on USY zeolite and application to free fatty acids esterification, Microporous Mesoporous Mater. 147 (2012) 142–148, https://doi.org/10.1016/j.micromeso.2011.06.008.

[38] S.S. Vieira, Z.M. Magriotis, N.A.V. Santos, A.A. Saczk, C.E. Hori, P.A. Arroyo, Biodiesel production by free fatty acid esterification using lanthanum (La^{3+}) and HZSM-5 based catalysts, Bioresour. Technol. 133 (2013) 248–255, https://doi.org/10.1016/j.biortech.2013.01.107.

[39] L. Peng, A. Philipaerts, B.F. Selsa, J.V. Noyen, F.D. Clippel, G.V. Tendeloo, P.A. Jacobs, B.F. Sels, Preparation of sulfonated ordered mesoporous carbon and its use for the esterification of fatty acids, Catal. Today 150 (2010) 140–146, https://doi.org/10.1016/j.cattod.2009.07.066.

[40] N. Kaur, A. Ali, Preparation and application of $Ce/ZrO_2–TiO_2/SO_4^{2-}$ as solid catalyst for the esterification of fatty acids, Renew. Energy 81 (2015) 421–431, https://doi.org/10.1016/j.renene.2015.03.051.

[41] A. Wang, H. Zhang, H. Li, S. Yang, Efficient production of methyl oleate using a biomass-based solid polymeric catalyst with high acid density, Adv. Polym. Technol. 2019 (2019), 4041631, https://doi.org/10.1155/2019/4041631.

[42] X. Zhang, H. You, Reaction conditions and kinetics for synthesizing methyl oleate, Org. Chem. Indian J. 10 (2014) 183–187.

[43] H. Yu, S. Niu, C. Lu, J. Li, Y. Yang, Sulfonated coal-based solid acid catalyst synthesis and esterification intensification under ultrasound irradiation, Fuel 208 (2017) 101–110, https://doi.org/10.1016/j.fuel.2017.06.122.

[44] M.N.B. Mohiddin, Y.H. Tan, Y.X. Seow, J. Kansedo, N.M. Mubarak, M.O. Abdullah, Y.S. Chan, K. Khalid, Evaluation on feedstock, technologies, catalyst and reactor for sustainable biodiesel production: a review, J. Ind. Eng. Chem. 98 (2021) 60–81, https://doi.org/10.1016/j.jiec.2021.03.036.

[45] N. Narkhede, A. Patel, Biodiesel production by esterification of oleic acid and transesterification of soybean oil using a new solid acid catalyst comprising 12-tungstosilicic acid and zeolite Hβ, Ind. Eng. Chem. Res. 52 (2013) 13637–13644, https://doi.org/10.1021/ie402230v.

[46] K. Ohto, Review of adsorbents incorporating calixarene derivatives used for metals recovery and hazardous ions removal: the concept of adsorbent design and classification of adsorbents, J. Inclusion Phenom. Macrocycl. Chem. 101 (2021 175-194), https://doi.org/10.1007/s10847-021-01053-x.

[47] D. Gendron, Vanillin: a promising biosourced building block for the preparation of various heterocycles, Front. Chem. 10 (2022), 949355, https://doi.org/10.3389/fchem.2022.949355.

[48] Y.S. Kurniawan, A.C. Imawan, Y.M. Stansyah, T.D. Wahyuningsih, Application of activated bentonite impregnated with PdO as green catalyst for acylation reaction of aromatic compounds, J. Environ. Chem. Eng. 9 (2021), 105508, https://doi.org/10.1016/j.jece.2021.105508.

[49] B.A. Roberts, G.W.V. Cave, C.L. Raston, J.L. Scott, Solvent-free synthesis of Calix[4]resorcinarenes, Green Chem. 3 (2001) 280–284, https://doi.org/10.1039/B104430N.

[50] B.Q. Ma, Y. Zhang, P. Coppens, The chair conformation of C-methylCalix[4]resorcinarene in a novel, stepped, supramolecular framework, CrystEngComm 3 (2001) 78–80, https://doi.org/10.1039/B103190M.

[51] A. Torres, B. Fuentes, K.E. Rodriguez, A. Brito, L. Diaz, Analysis of the content of fatty acid methyl esters in biodiesel by Fourier-transform infrared spectroscopy: method and comparison with gas chromatography, J. Am. Oil Chem. Soc. 97 (2020) 651–661, https://doi.org/10.1002/aocs.12350.

[52] K.V. Kumar, K. Porkodi, F. Rocha, Langmuir-Hinshelwood kinetics – a theoretical study, Catal. Commun. 9 (2008) 82–84, https://doi.org/10.1016/j.catcom.2007.05.019.

[53] M. Raita, W. Kiatkittipong, N. Laosiripojana, V. Champreda, Kinetic study on esterification of palmitic acid catalyzed by glycine-based crosslinked protein coated microcrystalline lipase, Chem. Eng. J. 278 (2015) 19–23, https://doi.org/10.1016/j.cej.2015.01.016.

[54] K. Saravanan, B. Tyagi, R.S. Shukla, H.C. Bajaj, Esterification of palmitic acid with methanol over template-assisted mesoporous sulfated zirconia solid acid catalyst, Appl. Catal. B Environ. 172–173 (2015) 108–115, https://doi.org/10.1016/j.apcatb.2015.02.014.

[55] D. Shin, Y. Kim, H.S. Moon, Fate and toxicity of spilled chemicals in groundwater and soil environment I: strong acids, Environ. Health Toxicol. 33 (2018), e2018019, https://doi.org/10.5620/eht.e2018019.

[56] D.A.C. Munguia, E. Tututi-Rios, A. Gutierrez-Alejandre, J.L. Rico, H. Gonzalez, Reaction study for the esterification of oleic acid over M-SBA-15-SO_3H (M=Al, Ti) catalysts, Energy Proc. 142 (2017) 590–596, https://doi.org/10.1016/j.egypro.2017.12.098.